

SEISMIC WAVE EFFECTS ON THE DYNAMIC RESPONSE OF BRIDGE FOUNDATIONS

Roberto Cairo¹, Giovanni Dente² and Stefano Dodaro³

^{1,2,3} University of Calabria, Department of Civil Engineering, Italy
e-mail: rcairo@unical.it, giovanni.dente@unical.it, stefanododaro@gmail.com

ABSTRACT: The dynamic response of structures to earthquake loading depends mainly on: the characteristics of the incident seismic waves; local site conditions, such as topographic irregularities and heterogeneity of the soils; the presence of stiff and heavy embedded foundations; the deformability of the soil supporting the structures. These phenomena can be relevant for bridges that usually have deep foundations and extent over considerable distances. In this paper the dynamic response of a bridge pier subjected to polarized shear waves is investigated. Different wave patterns are considered and the corresponding free-field ground motion is calculated with reference to a linear elastic halfspace. The pier is founded on a rigid caisson and soil-structure interaction is solved using the Winkler type model developed by Gerolymos and Gazetas.

KEYWORDS: Inclined waves; kinematic interaction; inertial interaction.

1 INTRODUCTION

The influence of soil-structure interaction (SSI) in the dynamic response of structures with massive or deep foundation (such as bridges) has been studied by many authors in the past [1-4]. Nevertheless, most of the foregoing research has been restricted to certain aspects of the SSI, without pointing out the relative importance and interdependency of the most important aspects of the phenomenon.

The seismic excitation experienced by structures is, definitely, a function of the earthquake source, travel paths of the seismic waves, local site conditions and, finally, soil-structure interaction [5-7].

The influence of local soil conditions on the nature of earthquake damage has been well established [8,9] and a number of techniques have been developed for ground response analysis. The major part of these methods deal with one-dimensional propagation of shear waves, considering both equivalent linear and nonlinear soil behavior. Nevertheless, one-dimensional analyses are useful for level or gently sloping sites, whereas for many other problems of interest the assumption of one-dimensional wave propagation is not acceptable as in the presence of irregular ground surface, heavy or stiff and embedded

structures.

A large number of field observations demonstrate that buildings located on hilltops suffer much more intensive damage than those located at the base of hills. Instrumental evidence reveals that topography affects largely the amplitude and frequency content of ground motion.

The importance of these effects has been shown to be rather sensitive to the characteristics of the incident wave field, such as wave type and propagation direction. Moreover, complex amplification and deamplification effects can cause significant differential motions along the ground surface. While the local variation of surface motion is usually negligible for commonly structures, this can be relevant for bridges that extend over considerable distances [10-12].

As a matter of fact, a first important feature of the dynamic soil-structure interaction (*kinematic interaction*) derives from the fact that the incident seismic waves are reflected and scattered by a relative rigid foundation and produce a base motion which is different from the motion occurring in the soil in the absence of the structure (the so-called *free-field motion*). The motion of the foundation may generally include rocking and torsional components in addition to the translational displacements. This type of interaction is strongly affected by the rigidity of the embedded foundation and the nature of the incoming seismic excitation consisting of non-vertically body and surface waves [13]. Generally, this *kinematic interaction* is strongly frequency-dependent being influenced by the wavelength of seismic waves compared to the dimension of the foundation elements. In the case of a shallow foundation, kinematic interaction is usually negligible [14], whereas should be in principle more relevant for drilled shafts and caissons, owing to the foundation size and embedment [15].

On the other end, the presence of a deformable soil deposit surrounding the foundation produces a longer fundamental period of oscillation with respect to that of the same structure founded on a rigid base and part of the vibration energy is dissipated into the soil by radiation of waves along with hysteretic action [16]. This is the result of an *inertial interaction* between the soil and the superstructure.

Although earthquake response of bridges should be evaluated with a direct analysis [2,17-19] capable of modelling the entire system composed of the superstructure, foundation and the supporting soil, to date the state of practice is usually restricted to a multistep approach [1,20,6,21,22], which makes use of the superposition theorem [23].

The so-called substructure method [24] consists of: (1) evaluating the free-field response of the site, that is the spatial and temporal variation of the ground motion before building the structure; (2) solving the kinematic interaction, i.e. the response to incident seismic waves of the soil-foundation system with the mass of the superstructure set equal to zero; (3) determining the inertial interaction, that is the response of the overall soil-foundation-superstructure

system to forces associated with accelerations arising from the kinematic interaction.

As a further simplification, kinematic interaction can be reduced to the evaluation of the motion at the base of the structure, disregarding the presence of the superstructure itself [25]. In the third step, kinematic motion is applied at the base of the superstructure in which the soil-foundation system is modelled with springs and dashpots (*dynamic impedances*) associated to each mode of vibrations [23].

A widely used approach to model the interaction between soil and deep foundations, for instance piles, is represented by the dynamic Winkler model [26]. It consists of a series of independent horizontal or vertical springs and dashpots continuously distributed along the surface of the pile. The other extremity of the springs and dashpots are connected to the free-field where the soil response, computed independently, is imposed. This method reveals quite accurate, despite the modest computational effort, and permits nonlinear behavior of the soil to be easily incorporated.

Gerolymos and Gazetas [27] developed a Winkler-type model for the seismic analysis of caisson foundations. Four types of springs and dashpots are used: distributed lateral springs and dashpots associated with the horizontal and rocking components of the motion of the caisson; springs and dashpots concentrated at the base of the caisson associated with the horizontal and rocking components of the motion.

This model was extended to consider nonlinearity of the soil-foundation interface [28,29]. Tsigginos et al. [21] used the Winkler-type model to study the seismic response of the foundation-structure system. Varun et al. [30] conducted a series of numerical simulations with the finite element method and furnished very simple expressions of the springs and dashpots of the model. This solution was used by Cairo and Dente [16] to analyze both kinematic and inertial interaction of the soil-foundation-superstructure system. Zhong and Huang [31] extended the Winkler type model to the case of composite caisson-piles foundations. The lateral response to external loads applied to caisson foundations was investigated by Karapiperis and Gerolymos [32] using nonlinear four-spring Winkler model.

In this paper, the original model developed by Gerolymos and Gazetas [27] is used to elucidate some important aspects of the dynamic behavior of a bridge pier founded on caisson subjected to harmonic SH and SV shear waves. The effects of different wave patterns on the dynamic response of the foundation as well as the superstructure are discussed.

2 FREE-FIELD SOIL RESPONSE

Filtering out the details, that can be found elsewhere [33], we consider harmonic plane waves, which propagate in the x-z plane in the interior of a

visco-elastic homogeneous halfspace (*Fig.1*). The halfspace is characterized by the shear modulus G , Poisson's ratio ν , mass density ρ and material damping ξ . Shear waves, that induce displacements in the planes perpendicular to the direction of propagation, are separated into two polarized waves: SH waves, whose displacement has only a y component, and SV waves, whose displacement is only in the x - z plane. In this framework, the displacements do not vary with y and can be written as a function only of x , z and time t . Moreover, the equation of motion associated with SH waves is independent from the equations associated with SV waves. On the contrary, SV waves form a coupled system with the longitudinal P waves (which induce oscillations in the direction of propagation), and both of them give rise to two components of displacement depending one from the other.

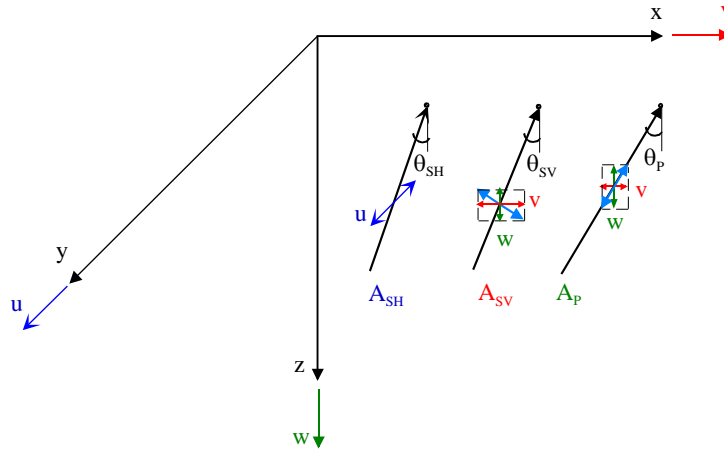


Figure 1. Plane body waves propagating in a halfspace

2.1 SH waves

Introducing the complex shear wave velocity $V_S = \sqrt{G(1 + 2i\xi)/\rho}$, that takes into account the material damping occurring in the halfspace, for SH waves with angle of incidence θ_{SH} measured from the vertical, the horizontal displacement in the y -direction is expressed as

$$u(x, z, t) = [A_{SH} \exp(ik_s m_z z) + B_{SH} \exp(-ik_s m_z z)] \exp(-ik_s m_x x) \exp(i\omega t) \quad (1)$$

with ω the circular frequency of the motion, $k_s = \omega/V_S$ the wave number, $m_x = \sin\theta_{SH}$ and $m_z = \cos\theta_{SH}$ the direction cosines, $i = \sqrt{-1}$, A_{SH} and B_{SH} the amplitude of the incident and reflected waves, respectively. At the free surface, $z=0$, the shear stress vanishes resulting in

$$B_{SH} = A_{SH} \quad (2)$$

Adopting a concise notation and using Euler's law, the horizontal displacement is formulated as

$$u(x, z, t) = u(z) \exp(-ik_s m_x x) \exp(i\omega t) \quad (3)$$

being

$$u(z) = 2A_{SH} \cos(k_s m_z z) \quad (4)$$

the amplitude of the SH wave propagating in the x-direction. The displacement amplitude at the free surface ($z=0$) follows

$$u_0 = 2A_{SH} \quad (5)$$

and it is independent of the angle of incidence θ_{SH} .

It should be pointed out that the terms $k_s m_x$ and $k_s m_z$ represent, respectively, the horizontal and vertical components of the wave vector, which describes the direction of wave propagation. The term $k_s m_x$ (usually named *apparent wave number*) can be also written as

$$k_s m_x = \frac{\omega}{V_s} \sin \theta_{SH} = \frac{\omega}{c} \quad (6)$$

where the ratio between V_s and m_x defines the so-called *apparent phase velocity* c , that is the velocity at which the plane wave appears to travel along the x-axis.

It is worth noting that the same relations are still valid in the case of a single surface soil layer as well as for the halfspace. Eq.(4) will be used to describe the free-field soil motion in the analysis of the kinematic interaction.

The ratio (*amplification function*) of the absolute value of the displacement amplitudes at the top of a homogeneous layer and at outcropping bedrock (Fig.2) is plotted in Fig.3 as a function of the circular frequency normalized with the depth of the layer and the shear wave velocity of the soil. Different angles of incidence of SH waves are considered. As can be seen, the free-field soil response tends to decrease increasing θ_{SH} . For $\theta_{SH}=80^\circ$, the free-field motion is deamplified into the soft layer. However, the fundamental frequency of the layer, i.e. the frequency at which the ground motion attains the maximum value, does not depend on the incident angle of the seismic waves.

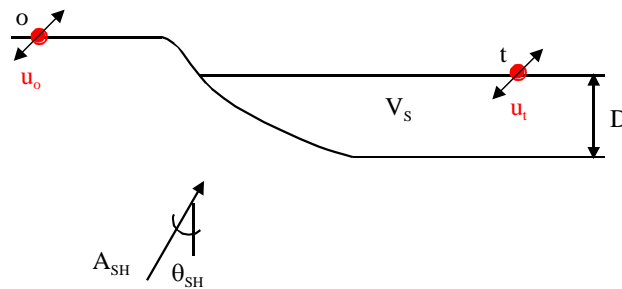


Figure 2. Homogeneous soil layer overlying a rigid bedrock subjected to inclined SH waves

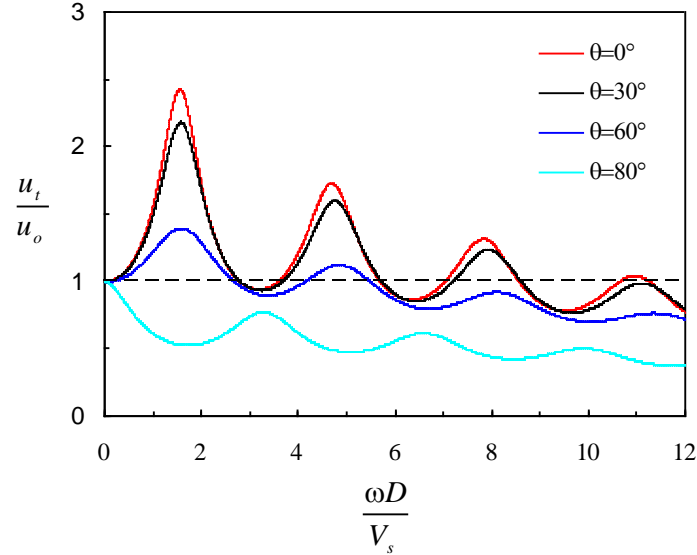


Figure 3. Amplification function for the soil deposit in Fig.2

2.2 SV waves

The scheme used for describing SH waves can be followed for analyzing the propagation of SV waves. It is worth noting that, in the virtue of Snell's law, the apparent phase velocity c (i.e. the apparent wave number) of both P and SV waves has to be the same. Therefore, the harmonic displacements caused by P and SV waves (Fig.1) have the form

$$v(x, z, t) = v(z) \exp(-ik_s m_x x) \exp(i\omega t) \quad (7a)$$

$$w(x, z, t) = w(z) \exp(-ik_s m_x x) \exp(i\omega t) \quad (7b)$$

being $m_x = \sin\theta_{SV}$, with the angle of incidence θ_{SV} measured from the vertical, and

$$v(z) = n_x [A_P \exp(ik_p n_z z) + B_P \exp(-ik_p n_z z)] - m_z [A_{SV} \exp(ik_s m_z z) - B_{SV} \exp(-ik_s m_z z)] \quad (8a)$$

$$w(z) = -n_z [A_P \exp(ik_p n_z z) - B_P \exp(-ik_p n_z z)] - m_x [A_{SV} \exp(ik_s m_z z) + B_{SV} \exp(-ik_s m_z z)] \quad (8b)$$

the amplitudes of the horizontal and vertical displacements associated with the waves traveling in the x-direction, respectively. In these equations, A_P and A_{SV} are the amplitudes of the incident P and SV waves, respectively, B_P and B_{SV} are the reflected ones, $m_z = \cos\theta_{SV}$, $n_x = \sin\theta_P$ and $n_z = \cos\theta_P$ are the direction cosines, $k_p = \omega/V_P$ the wave number, where V_P is the longitudinal wave velocity. The ratio between the shear wave velocity V_S and V_P can be written in terms of Poisson's ratio as

$$\delta = \frac{V_S}{V_P} = \sqrt{\frac{1-2\nu}{2(1-\nu)}} \quad (9)$$

Introducing the boundary conditions at the free surface of the halfspace (i.e. normal and shear stresses equal to 0), the amplitudes of the reflected waves can be expressed as a function of the incident waves. To study the kinematic response of the foundation to obliquely shear waves, the presence of the incident P wave is neglected, that is $A_P=0$. Therefore, the following ratios are derived

$$\frac{B_{SV}}{A_{SV}} = \frac{-\sin^2(2\theta_{SV}) + \delta^2 \cos(2\theta_{SV}) \cos(2\theta_P)}{\sin^2(2\theta_{SV}) + \delta^2 \cos(2\theta_{SV}) \cos(2\theta_P)} \quad (10a)$$

$$\frac{B_P}{A_{SV}} = \frac{2\delta \sin(2\theta_{SV}) \cos(2\theta_{SV})}{\sin^2(2\theta_{SV}) + \delta^2 \cos(2\theta_{SV}) \cos(2\theta_P)} \quad (10b)$$

It should be noticed that an obliquely incident SV wave generates both SV and P waves reflected only if θ_{SV} is lesser than a critical angle given by

$$\theta_{cr} = \arccos \delta \quad (11)$$

The critical angle depends only on Poisson's ratio. For $\nu=1/3$, $\theta_{cr}=60^\circ$.

Substituting in Eq.(8a) the ratios above derived (Eq.10), the horizontal displacement amplitude at the free surface ($z=0$) of the halfspace can be obtained

$$v_0 = 2A_{SV} \frac{\cos(\theta_{SV}) \sin(2\theta_{SV})}{\sin^2(2\theta_{SV}) + \delta^2 \cos(2\theta_{SV}) \cos(2\theta_P)} \quad (12)$$

As can be noticed, the horizontal motion at the free surface of the halfspace induced by an obliquely incident SV wave depends strongly on the angle of incident θ_{SV} [34,35].

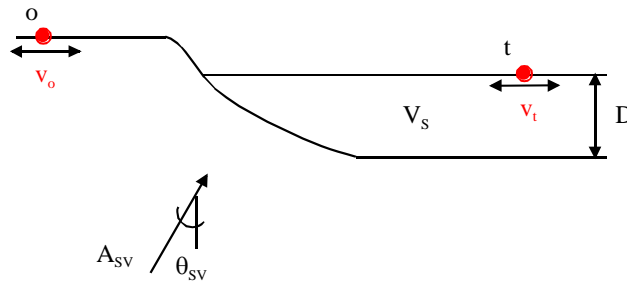


Figure 4. Homogeneous soil layer overlying a rigid bedrock subjected to inclined SV waves

The horizontal amplification function of the soil layer depicted in Fig.4 is discussed. In contrast to SH waves, the horizontal displacement at the free surface depends strongly on the incident angle of SV waves (Fig.5), especially when θ_{SV} is greater than the critical angle θ_{cr} . At the fundamental frequency of the layer, the maximum response of the soil is attained for waves inclined of

60°. In this case, as when $\theta_{sv}=80^\circ$, a second mode of vibration appears to be much important, although it corresponds to a medium/high range of frequencies.

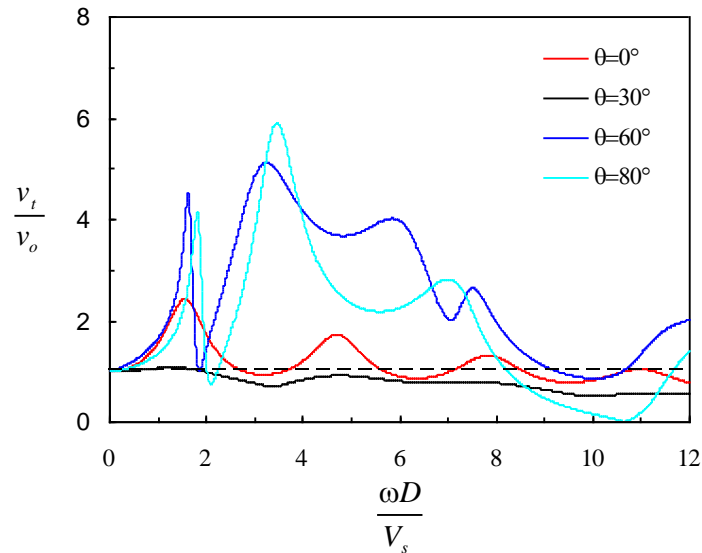


Figure 5. Amplification function for the soil deposit in Fig.4

3 BRIDGE-SOIL MODEL

A rigorous treatment of the seismic behavior of bridge piers would require evaluation of the inelastic response of the superstructure. However, an attempt is made herein to clarify important features of the dynamic response of a simple soil-superstructure model (Fig.6), generally used to analyze in a very simple manner single-pier bridges. It consists of a single-degree-of-freedom structure (SDOF) with lumped mass m , height h , elastic stiffness k and damping ratio ξ_s . The compliance of the base of the SDOF is represented by the horizontal impedance S_{hh} , the rocking impedance S_{rr} and the coupled impedance S_{hr} , associated with each mode of vibrations of the rigid foundation. The kinematic motion FIM (*foundation input motion*) is directly applied at the base.

In the following, the evaluation of the FIM, that is the kinematic response of the foundation, as well as the determination of dynamic impedances S_{ij} of the soil-foundation system are performed using the linear four-spring Winkler model proposed by Gerolymos and Gazetas [27].

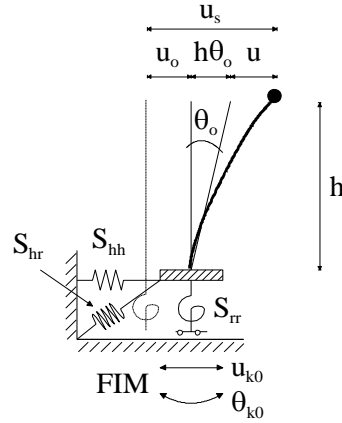


Figure 6. Single-degree-of-freedom structure resting on soft soil

3.1 Four-spring Winkler model

The Winkler type model developed for the dynamic response of rigid caisson foundations consists of four types of linear springs and dashpots: two distributed translational and rotational impedances on the shaft of the caisson, two concentrated translational and rotational impedances at the base (Fig.7b). The spring coefficient k_j at the shaft of the caisson (K_j at its base) takes into account the stiffness and inertia of the supporting soil and is therefore termed dynamic stiffness; c_j (or C_j) is the dashpot coefficient which reflects the radiation and material damping generated in the system. As known, in the frequency domain ω each dynamic impedance component j can be written in complex notation as

$$\bar{k}(\omega) = k(\omega) + i\omega c(\omega) \quad (13)$$

The dynamic equilibrium of the shear forces and moments with respect to the base of the caisson is expressed in the usual matrix notation

$$([\bar{K}] - \omega^2[M])\{u\} = \{P\} \quad (14)$$

in which $[\bar{K}]$ and $[M]$ are the impedance and mass matrices of the caisson referred to the base, respectively; $\{u\}$ contains the horizontal displacement of the base and the rotation of the caisson; $\{P\}$ is the load vector.

The impedance matrix of the soil-foundation system adopted takes the following form [27]

$$[\bar{K}] = \begin{bmatrix} \bar{K}_h + \bar{k}_x D & \bar{k}_x D^2 / 2 \\ \bar{k}_x D^2 / 2 & \bar{K}_r + \bar{k}_\theta D + \bar{k}_x D^3 / 3 \end{bmatrix} \quad (15)$$

being D the depth of embedment of the caisson.

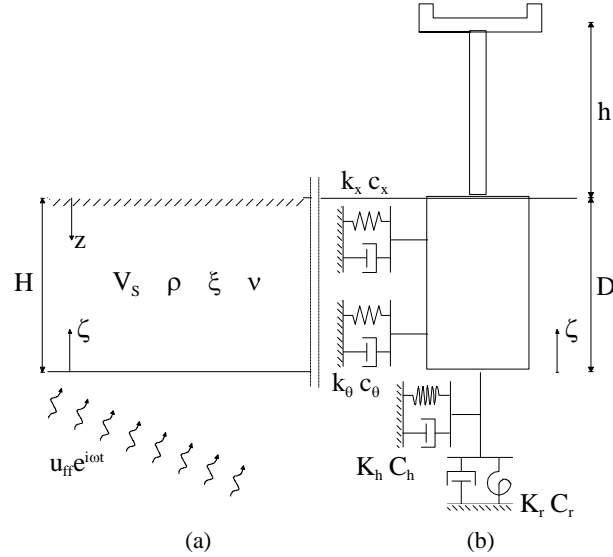


Figure 7. Free-field soil (a) and bridge-pier on Winkler caisson foundation (b)

Considering a rigid block foundation of mass m_0 and mass moment of inertia about the center of gravity I_0 , the mass matrix results [27]

$$[M] = \begin{bmatrix} m_0 & m_0 D/2 \\ m_0 D/2 & I_0 + m_0 D^2/4 \end{bmatrix} \quad (16)$$

In general, the dynamic impedances of rigid caissons come indirectly from studies of the dynamic response of embedded footings [36,37]. Defining the impedance matrix of the embedded footing as

$$\tilde{K}_{emb} = \begin{bmatrix} \tilde{K}_{HH} & \tilde{K}_{MH} \\ \tilde{K}_{MH} & \tilde{K}_{MM} \end{bmatrix} \quad (17)$$

the terms of which can be found in Appendix I, the lateral springs k_j and dashpots c_j of the equivalent Winkler model can be derived by equating the translational and rocking components of the impedance matrix in Eq. (15) with the corresponding terms in \tilde{K}_{emb} [27]. The following expressions thus result

$$\bar{k}_x = \frac{1}{D} (\tilde{K}_{HH} - \bar{K}_h) \quad (18a)$$

$$\bar{k}_\theta = \frac{1}{D} \left(\tilde{K}_{MM} - \bar{K}_r - \bar{k}_x \frac{D^3}{3} \right) = \frac{1}{D} (\tilde{K}_{MM} - \bar{K}_r) - \frac{D}{3} (\tilde{K}_{HH} - \bar{K}_h) \quad (18b)$$

According to Tsigginos et al. [21], the impedances of the base of the caisson can be selected as the springs K_j and dashpots C_j coefficients of a surface foundation on halfspace or on a soil stratum underlain by a homogeneous halfspace (Appendix I)

$$\bar{K}_x = K_{H_{surf}} + i\omega C_{H_{surf}} \quad (19a)$$

$$\bar{K}_r = K_{M_{surf}} + i\omega C_{M_{surf}} \quad (19b)$$

Once all the springs and dashpots of the Winkler model are defined, the impedance matrix S referred to the top of the caisson can be obtained with a rapid coordinate transformation of Eq.(15), that is

$$[S] = \begin{bmatrix} S_{hh} & S_{hr} \\ S_{hr} & S_{rr} \end{bmatrix} = \begin{bmatrix} \bar{K}_{11} & \bar{K}_{12} - D\bar{K}_{11} \\ \bar{K}_{12} - D\bar{K}_{11} & \bar{K}_{22} - 2D\bar{K}_{12} + D^2\bar{K}_{22} \end{bmatrix} \quad (20)$$

4 KINEMATIC INTERACTION

The seismic waves propagating into the soil impose forces and moments at the supports of the distributed springs and dashpots along the caisson height and at the concentrated impedances of the base (Fig. 7a), which lead to the following load vector [27]

$$\{P\} = \left\{ \begin{array}{l} \int_0^D \bar{k}_x u_{ff}(\zeta) d\zeta + \bar{K}_h u_{ff}(\zeta=0) \\ \int_0^D \bar{k}_x u_{ff}(\zeta) \zeta d\zeta + \int_0^D \bar{k}_\theta u'_{ff}(\zeta) d\zeta + \bar{K}_r u'_{ff}(\zeta=0) \end{array} \right\} \quad (21)$$

where u_{ff} and u'_{ff} are the free-field displacement and its derivative with respect to ζ measured upwards from the base of the caisson, respectively. The kinematic response of the caisson is obtained from the dynamic equilibrium equation (Eq.14), which gives the horizontal displacement of the base of the caisson and its rotation. The foundation input motion at the top of the caisson u_{ko} (along with rotation θ_{ko}) follows.

4.1 Solution for SH waves

In the case of obliquely SH waves, Eq.(4) is used to calculate the free-field displacement and its derivative in Eq.(21). Assuming the lateral spring \bar{k}_x and dashpot \bar{k}_θ to be constant into the layer considered, the translational and rotational components of the load vector in Eq.(21) can be written as

$$P_{b1} = \bar{k}_x p_1 + \bar{K}_h u_{ff0} \quad (22a)$$

$$P_{b2} = \bar{k}_x p_2 + \bar{k}_\theta p_3 + \bar{K}_r u'_{ff0} \quad (22b)$$

in which

$$p_1 = u_0 \frac{\sin(k_s m_z D)}{k_s m_z} \quad (23a)$$

$$p_2 = u_0 \frac{1 - \cos(k_s m_z D)}{k_s^2 m_z^2} \quad (23b)$$

$$p_3 = u_0 [1 - \cos(k_s m_z D)] \quad (23c)$$

$$u_{ff0} = u_0 \cos(k_s m_z D) \quad (24a)$$

$$u'_{ff0} = u_0 k_s m_z \sin(k_s m_z D) \quad (24b)$$

being u_0 the amplitude of the horizontal motion at the free surface (Eq.5), u_{ff0} and u'_{ff0} the free-field displacement and its derivative at the base of the caisson, respectively.

4.2 Solution for SV waves

As previously done for SH waves, the amplitude of the free-field displacement u_{ff0} at the base of the caisson and its derivative u'_{ff0} are determined for inclined SV waves, using Eq.(8a) in the case of a homogeneous soil layer. The following expressions result

$$u_{ff0} = m_z(-A_{SV}a_{SV} + B_{SV}b_{SV}) + n_x B_P b_P \quad (25a)$$

$$u'_{ff0} = i k_s m_z^2 (A_{SV}a_{SV} + B_{SV}b_{SV}) + i k_p n_z n_x B_P b_P \quad (25b)$$

in which

$$a_{SV} = \cos(k_s m_z D) + i \sin(k_s m_z D) \quad (26a)$$

$$b_{SV} = \cos(k_s m_z D) - i \sin(k_s m_z D) \quad (26b)$$

$$b_P = \cos(k_p n_z D) - i \sin(k_p n_z D) \quad (26c)$$

$$A_{SV} = \frac{\sin^2(2\theta_{SV}) + \delta^2 \cos(2\theta_{SV}) \cos(2\theta_P)}{2 \cos(\theta_{SV}) \sin(2\theta_{SV})} v_0 \quad (27a)$$

$$B_{SV} = \frac{-\sin^2(2\theta_{SV}) + \delta^2 \cos(2\theta_{SV}) \cos(2\theta_P)}{2 \cos(\theta_{SV}) \sin(2\theta_{SV})} v_0 \quad (27b)$$

$$B_P = \frac{\delta \sin(4\theta_{SV})}{2 \cos(\theta_{SV}) \sin(2\theta_{SV})} v_0 \quad (27c)$$

The loading coefficients in Eq.(22) can be simply written as

$$p_1 = -i \frac{A_{SV}(1-a_{SV}) + B_{SV}(1-b_{SV})}{k_s} - i \frac{B_P n_x (1-b_P)}{k_p n_z} \quad (28a)$$

$$p_2 = -i \frac{D(A_{SV} + B_{SV})}{k_s} - \frac{A_{SV}(1-a_{SV}) - B_{SV}(1-b_{SV})}{k_s^2 m_z} + \frac{B_P n_x (1-b_P)}{k_p^2 n_z^2} - i \frac{B_P n_x D}{k_p n_z} \quad (28b)$$

$$p_3 = -A_{SV}(1-a_{SV}) + B_{SV}(1-b_{SV}) + B_P n_x (1-b_P) \quad (28c)$$

4.3 Kinematic response factors

Kinematic interaction is usually expressed in terms of the kinematic response factors, that quantify the dynamic response of the foundation to the propagation of waves into the surrounding soil. Denoting with u_{ko} the horizontal displacement at the top of the caisson and θ_{ko} the rotational component, calculated with Eq.(14), the kinematic response factors are defined as the absolute values of the following normalized ratios

$$\eta_{eff} = \frac{u_{ko}}{u_{ffD}} \quad (29a)$$

$$\theta_{eff} = \frac{\theta_{k0}}{u_{ffD}} D \quad (29b)$$

in which u_{ffD} is the free-field motion at the base of the layer and D the thickness of the layer.

The kinematic response factors are thus calculated with the aforementioned approach. A square prismatic caisson foundation of width $B=4$ m and height $D=6$ m, embedded in a uniform elastic soil stratum overlying a homogeneous halfspace is considered. The mass m_o of the caisson is neglected for sake of simplicity. The soil layer has shear modulus $G=50$ MPa, Poisson's ratio $\nu=0.3$, mass density $\rho=1.8$ Mg/m³, internal damping $\xi=5\%$.

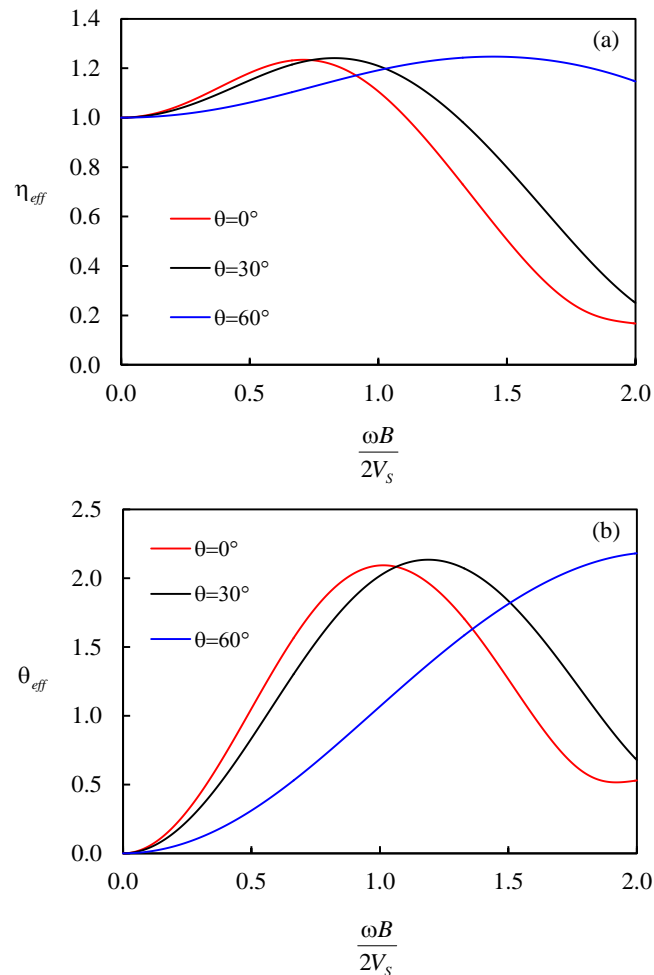


Figure 8. Kinematic response factor of the caisson to obliquely incident SH waves: (a) horizontal and (b) rotational components

Figure 8 shows the kinematic response of the caisson plotted versus the dimensionless frequency $a_0 = \omega B / 2V_s$ for obliquely incident SH waves. At low and medium frequencies, the kinematic response of the caisson u_{ko} is greater than the surface free-field displacement (Fig.8a), especially for vertically ($\theta_{SH} = 0^\circ$) or slightly obliquely ($\theta_{SH} = 30^\circ$) incident SH waves. This is caused by the rapid development of the rocking component θ_{ko} in the same frequency range (Fig.8b). At higher frequencies, u_{ko} tends to attenuate rapidly and becomes minor than the movement of the ground, although significant values of the rocking motion remain. For SH waves inclined of $\theta_{SH} = 60^\circ$ the rocking component (Fig.8b) develops gradually with frequency and the horizontal displacement is less pronounced, although remains above unity for all the frequency range (Fig.8a).

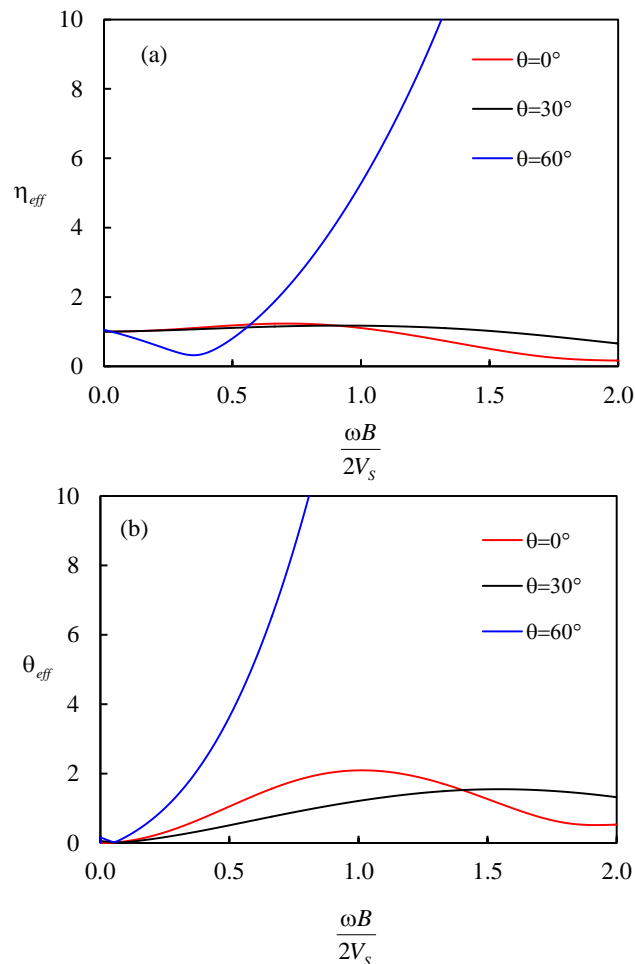


Figure 9. Kinematic response factor of the caisson to obliquely incident SV waves: (a) horizontal and (b) rotational components

By comparisons with previous results obtained by Cairo and Dente [16] for vertical S waves, taking into account the mass of the foundation would determine an increase of the kinematic factors. Only when the caisson is founded directly on a bedrock, the influence of the mass of the caisson has expected to be practically negligible.

Kinematic response for SV waves is represented in *Fig.9*. For $\theta_{SV}=0^\circ$ and $\theta_{SV}=30^\circ$, the kinematic factors show almost the same trend as for SH waves, although kinematic interaction reveals less important for $\theta_{SV}=30^\circ$ with respect to S waves vertically incident. On the contrary, SV waves inclined at 60° induce a very important kinematic effect in the foundation, also at very low frequencies, especially for the rotational component (*Fig.9b*).

5 INERTIAL INTERACTION

In the inertial interaction, the soil-foundation system is modeled through the dynamic impedances computed at the top of the caisson (*Fig.6*). By means of the coordinate transformation performed in Eq.(20), the following expressions are obtained

$$S_{hh} = \bar{K}_h + \bar{k}_x D \quad (30a)$$

$$S_{hr} = S_{rh} = -\bar{K}_h D - \bar{k}_x D^2 / 2 \quad (30b)$$

$$S_{rr} = \bar{K}_r + \bar{K}_h D^2 + \bar{k}_0 D + \bar{k}_x D^3 / 3 \quad (30c)$$

The response of the bridge pier to the foundation input motion with amplitude u_{k0} and θ_{k0} is thus evaluated solving the dynamic equilibrium of the idealized structural system sketched in *Fig.6*. The foundation has two degrees of freedom consisting of the horizontal displacement with amplitude u_0 and rocking with amplitude θ_0 . The elastic horizontal displacement of the top mass relative to the base mass has amplitude u . The total displacement amplitude of the superstructure results $u_s = u_0 + h\theta_0 + u$.

Formulating dynamic equilibrium of the mass of the superstructure and the translational and rotational equilibrium of the whole system yields

$$(-\omega^2 m + k)u - \omega^2 m u_0 - \omega^2 m h \theta_0 = \omega^2 m (u_{k0} + h \theta_{k0}) \quad (31a)$$

$$\begin{aligned} -\omega^2 m u - \omega^2 (m + m_0) u_0 - \omega^2 m h \theta_0 + S_{hh} u_0 + S_{hr} \theta_0 \\ = \omega^2 (m + m_0) u_{k0} + \omega^2 m h \theta_{k0} \end{aligned} \quad (31b)$$

$$\begin{aligned} -\omega^2 m h u - \omega^2 m h u_0 - \omega^2 (m h^2 + I_t) \theta_0 + S_{rh} u_0 + S_{rr} \theta_0 \\ = \omega^2 m h (u_{k0} + h \theta_{k0}) + \omega^2 I_t \theta_{k0} \end{aligned} \quad (31c)$$

being I_t the total centroidal moment of inertia of the masses.

These equations can be rearranged in matrix form as

$$\begin{aligned}
& \begin{bmatrix} -1 + \frac{1+2i\xi_s}{(\omega/\omega_s)^2} & -1 & -1 \\ -1 & \frac{S_{hh}}{\omega^2 m} - (1+\bar{m}) & \frac{S_{hr}}{\omega^2 mh} - 1 \\ -1 & \frac{S_{hr}}{\omega^2 mh} - 1 & \frac{S_{rr}}{\omega^2 mh^2} - \left(1 + \frac{I_t}{mh^2}\right) \end{bmatrix} \begin{Bmatrix} u \\ u_0 \\ h\theta_0 \end{Bmatrix} \\
& = \begin{Bmatrix} 1 \\ 1+\bar{m} \\ 1 \end{Bmatrix} u_{k0} + \begin{Bmatrix} 1 \\ 1 \\ 1 + \frac{I_t}{mh^2} \end{Bmatrix} h\theta_{k0} \quad (32)
\end{aligned}$$

in which $\bar{m} = m_0/m$.

In the following, the dynamic response of a bridge pier subjected to the foundation input motion derived in the previous section is examined. The superstructure is idealized as a SDOF with lumped mass $m=1200$ Mg, moment of inertia $I=64$ m⁴, height $h=30$ m and damping ratio $\xi_s=5\%$. For fixed-base response, the structure has undamped natural frequency $\omega_s=7.01$ rad/s that corresponds to 1.12 Hz.

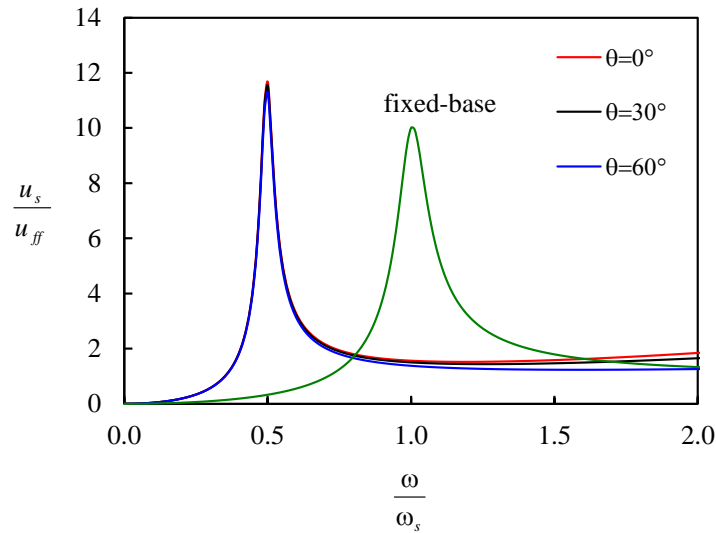


Figure 10. Inertial response of the structure versus the frequency ratio: base motion induced by SH waves

The total displacement amplitude of the structure normalized by the amplitude

of the surface free-field displacement is presented in *Fig.10* and *Fig.11*, as a function of the frequency ratio ω/ω_s of the excitation frequency to the fixed-base natural frequency of the structure. The solution disregarding the soil, i.e. for fixed-base structure, is also plotted. This corresponds to the well-known frequency response curve with the peak of $1/2\xi_s$ occurring at a *tuning ratio* $\omega/\omega_s=1$.

Under the base motions produced by SH waves, the peak responses (*Fig.10*) of the coupled soil-structure system under examination result greater than that of the same structure on a rigid base and occur at a lower frequency, corresponding to a more flexible system. The influence of θ_{SH} is practically irrelevant, although vertical incident waves produce a slightly higher response of the structure. The curves appear also less broad, indicating that the damping is smaller. This is probably due to the slenderness of the superstructure and the relative dimensions of the foundation [15].

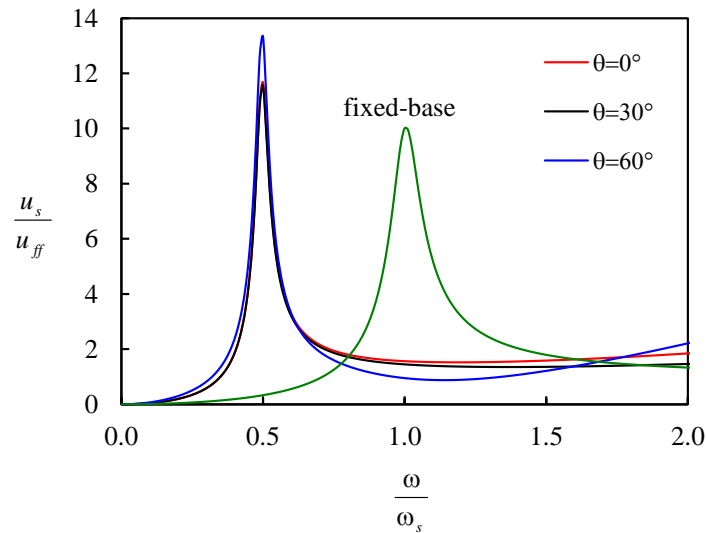


Figure 11. Inertial response of the structure versus the frequency ratio: base motion induced by SV waves

The same tendency is observed for base motions provided by SV waves (*Fig. 11*). However, for waves inclined at 60° the structure exhibits the maximum response, owing to a higher amplitude of the motion imposed at the foundation (*Fig.9*).

In the high frequency range, the effects of inertial interaction are expected to be more significant as a consequence of the large values of the rocking component of FIM (*Fig.8b* and *Fig.9b*). These aspects are not shown herein, and can be found in Cairo and Dente [16].

6 CONCLUDING REMARKS

In this paper the effects of wave pattern induced by polarized shear waves propagating into an elastic halfspace on the dynamic response of a bridge pier supported by a rigid caisson are highlighted and discussed. Obliquely incident harmonic SH and SV waves are analysed and the elasto-dynamic solutions are used to evaluate the free-field motion within a single soil layer resting on a rigid bedrock or an elastic halfspace. Soil-structure interaction is solved with the substructure method and the four-spring Winkler model [27] is employed to represent the behavior of the soil-foundation system. The pier is modeled as a one-degree-of-freedom system consisting of a mass concentrated at the top of a visco-elastic beam. The steady-state response of the entire system excited by obliquely SH and SV waves is evaluated by decomposing the problem into kinematic and inertial responses.

The obtained results permit the following remarks to be drawn:

- The free-field response of the soil depends not only on the frequency of the motion but also on the angle of incidence θ of the shear waves;
- The more the direction of propagation of the SH waves deviates from the vertical, the more the amplification function decreases, over the whole range of frequency;
- The amplification of the horizontal motion for incident SV waves is strongly influenced by the angle of incidence, being larger or smaller than for the vertical case;
- The fundamental frequency of the soil layer does not vary with θ ;
- The kinematic interaction for a rigid caisson foundation is characterized by a significant rocking motion, which leads to a lateral displacement of the base greater than the surface free-field movement in a wide frequency range;
- The foundation input motion depends markedly on the wave pattern imposed by the free-field soil. The influence of inclined SV waves is more pronounced;
- The soil deformability can play an important role in the kinematic response of the foundation as well as in the total response of the superstructure;
- The fundamental natural frequency of the soil-structure system is always reduced with respect to that calculated ignoring SSI;
- The peak response of the structure can be larger or smaller compared to the same fixed-base structure, depending on the compliance of the soil, the slenderness of the superstructure and the dimensions of the foundation.

Although the used approaches are based on some approximate assumptions, the conclusions drawn in the present study can be of help in predicting the dynamic response of bridges on deep foundations, or in interpreting the results of more rigorous numerical studies. It should be pointed out that all the presented issues are rigorously valid under the assumption of linear elastic behaviour of the soil.

APPENDIX**Translational impedance** (rectangular base, $B \times L$)

$$\tilde{K}_{HH} = K_{HH} + i\omega C_{HH}$$

$$K_{HH} = K_{Hemb} \chi_{Hemb}$$

$$\chi_{Hemb} = 1 + a_0 \left(\frac{D}{B}\right) \left\{ \left[0.08 - 0.0074 \left(\frac{D}{B}\right) \right] a_0^2 - \left[0.31 - 0.0416 \left(\frac{D}{B}\right) \right] a_0 - 0.0442 \left(\frac{D}{B}\right) + 0.14 \right\}$$

$$K_{Hemb} = K_{Hsurf} \left(1 + 0.15 \sqrt{\frac{2D}{B}} \right) \left[1 + 0.52 \left(\frac{8D(B+L)}{BL^2} \right)^{0.4} \right]$$

$$K_{Hsurf} = \frac{GL}{1-\nu} \left(2 + 2.75 \left(\frac{B}{L}\right)^{0.85} \right)$$

$$C_{HH} = C_{Hsurf} + 2\rho V_s B D \left(B + \frac{3.4L}{\pi(1-\nu)} \right)$$

$$C_{Hsurf} = \rho V_s B L \bar{c}_y$$

$$\bar{c}_y \approx 1$$

Coupled translational-rotational impedance

$$\tilde{K}_{HM} \approx \frac{1}{3} d \tilde{K}_{HH}$$

Rotational impedance (rectangular base, $B \times L$)

$$\tilde{K}_{MM} = K_{MM} + i\omega C_{MM}$$

$$K_{MM} = K_{Memb} \chi_{Memb}$$

$$\chi_{Memb} = 1 - 0.3a_0$$

$$K_{Memb} = K_{Msurf} \left(1 + 1.26 \cdot \left(\frac{2D}{B}\right) + \sqrt{\frac{B}{L}} \right)$$

$$K_{Msurf} = \frac{G}{1-\nu} \left(\frac{LB^3}{12} \right)^{0.75} \left(\frac{L}{B} \right)^{0.25} \left(2.4 + 0.5 \frac{B}{L} \right)$$

$$C_{MM} = C_{Msurf} + \rho \bar{c}_1 \frac{DLB^2}{6} \left[4 \frac{3.4V_s}{\pi(1-\nu)} \left(\frac{D}{B}\right)^2 + 3V_s + V_s \left(\frac{B}{L}\right) \left(1 + 4 \left(\frac{D}{B}\right)^2 \right) \right]$$

$$C_{Msurf} = \rho \frac{3.4 V_s}{\pi(1-\nu)} \frac{LB^3}{12} \bar{c}_{rx}$$

$$\bar{c}_{rx} = \frac{0.66 a_0^2}{(1 + 1.2 a_0^2)}$$

$$\bar{c}_1 = 0.25 + 0.65 \sqrt{a_0} \left(\frac{2D}{B} \right)^{-0.25}$$

REFERENCES

- [1] Mylonakis, G, Nikolaou, A, Gazetas, G, "Soil-pile-bridge seismic interaction: kinematic and inertial effects. Part 1: soft soil", *Earthq. Engng. Struct. Dyn.*, 26, pp. 337-359, 1997.
- [2] Kappos, AJ, Manolis, GD, Moschonas, IF, "Seismic assessment and design of R/C bridges with irregular configuration, including SSI effects", *Engineering Structures*, 24, pp. 1337-1348, 2002.
- [3] Spyarakos, C, Loannidis, G, "Seismic behavior of a post-tensioned integral bridge including soil-structure interaction (SSI)", *Soil Dynamics and Earthquake Engineering*, 23, pp. 53-63, 2003.
- [4] Spyarakos, CC, Xu, C, "Dynamic analysis of flexible massive strip-foundations embedded in layered soils by hybrid BEM-FEM", *Computers and Structures*, 82, pp. 2541-2550, 2004.
- [5] Stewart, JP, Fenves, GL, Seed, RB, "Seismic soil-structure interaction in buildings. I: analytical methods", *Journal of Geotechnical and Geoenvironmental Engineering*, ASCE, 125(1), pp. 26-37, 1999.
- [6] Sextos, AG, Pitilakis, KD, Kappos, AJ, "Inelastic dynamic analysis of RC bridges accounting for spatial variability of ground motion, site effects and soil-structure interaction phenomena. Part 2: Parametric study", *Earth. Eng. and Struct. Dyn.*, 32, pp. 629-652, 2003.
- [7] Mavroeidis, GP, Dong, G, Papageorgiou, AS, "Near-fault ground motions, and the response of elastic and inelastic single-degree-of-freedom (SDOF) systems", *Earthquake Engineering and Structural Dynamics*, 33, 1023-1049, 2004.
- [8] Elnashai, AS, McClure, DC, "Effect of modelling assumptions and input motion characteristics on seismic design parameters of RC bridge piers", *Earthquake Engineering and Structural Dynamics*, 25, pp. 435-463, 1996.
- [9] Mylonakis, G, Syngros, C, Gazetas, G, Tazoh, T, "The role of soil in the collapse of 18 piers of Hanshin expressway in the Kobe earthquake", *Earth. Eng. and Struct. Dyn.*, 35, pp. 547-575, 2006.
- [10] Dumanogluid, AA, Soylul, K, "A stochastic analysis of long span structures subjected to spatially varying ground motions including the site-response effect", *Engineering Structures*, 25, pp. 1301-1310, 2003.
- [11] Chouw, N, Hao, H, "Significance of SSI and nonuniform near-fault ground motions in bridge response I: Effect on response with conventional expansion joint", *Engineering Structures*, 30, pp. 141-153, 2008.
- [12] Bi, K, Hao, H, "Numerical simulation of pounding damage to bridge structures under spatially varying ground motions", *Engineering Structures*, 46, pp. 62-76, 2013.
- [13] Gazetas, G, *Soil dynamics: an overview*. Dynamic behaviour of foundations and buried structures, Banerjee & Butterfield (eds), Elsevier Appl. Sc., pp. 1-43, 1987.
- [14] Cairo, R, Dente, G, "Analisi semplificata dell'interazione dinamica terreno-struttura per le fondazioni superficiali", *Fondazioni superficiali e profonde*, V CNRIG, Bari, Hevelius edizioni, Benevento, vol. 1, pp. 69-81, 2006 (in Italian).
- [15] Cairo, R, Conte, E, "L'interazione terreno-struttura nella risposta sismica di ponti con fondazioni profonde", XXV CNG - La Geotecnica nella difesa del territorio e delle

- infrastrutture dalle calamità naturali, AGI, vol. 1, pp. 77-93, 2014 (in Italian).
- [16] Cairo, R, Dente, G, “Aspects of the soil-structure interaction – The dynamic response of bridge piers on caisson foundations”, *International Journal of Bridge Engineering*, vol. 3, n. 1, pp. 1-9, 2015.
- [17] Zafeirakos, A, Gerolymos, N, Gazetas, G, “The role of soil and interface nonlinearities on the seismic response of caisson supported bridge piers”, *Proc. 5th International Conference on Geotechnical Earthquake Engineering*, Santiago (Chile), 2011.
- [18] Loli, M, Bransby, MF, Anastasopoulos, I, Gazetas, G, “Interaction of caisson foundations with a seismically rupturing normal fault: centrifuge testing versus numerical simulation”, *Géotechnique*, 62(1), pp. 33-53, 2012.
- [19] Zafeirakos, A, Gerolymos, N, “Seismic performance of caisson supported piers”, *Proc. 2nd International Conference on Performance-based Design in Earthquake Geotechnical Engineering*, Taormina, pp. 900-914, 2012.
- [20] Zhang, J, Makris, N, “Seismic response analysis of highway overcrossings including soil-structure interaction”, *Earthquake Engineering and Structural Dynamics*, 31, pp. 1967-1991, 2002.
- [21] Tsigginos, C, Gerolymos, N, Assimaki, D, Gazetas, G, “Seismic response of bridge pier on rigid caisson foundation in soil stratum”, *Earthq. Eng. and Eng. Vib.*, Vol. 7, No. 1, pp. 33-44, 2008.
- [22] Carbonari, S, Dezi, F, Leoni, G, “Seismic soil-structure interaction in multi-span bridges: application to a railway bridge”, *Earthquake Engineering and Structural Dynamics*, 40, pp. 1219-1239, 2011.
- [23] Kausel, E, Roësset, JM, “Soil structure interaction for nuclear containment structures”, *Proceedings of ASCE, Power Division Speciality Conference*, Boulder, Colorado, 1974.
- [24] Gazetas, G, Mylonakis, G, “Seismic soil-structure interaction: new evidence and emerging issues”, *Geotech. Spec. Publ. No. 75, 2*, ASCE, pp. 1119-1174, 1998.
- [25] Whitman, RV, Bielak, J, *Foundations*, Design of earthquake resistant structures. Ed. E. Rosenblueth, Pentech Press, Plymouth, pp. 223-260, 1980.
- [26] Kavvadas, M, Gazetas, G, “Kinematic seismic response and bending of free-head piles in layered soils”, *Géotechnique*, 43(2), pp. 207-222, 1993.
- [27] Gerolymos, N, Gazetas, G, “Winkler model for lateral response of rigid caisson foundations in linear soil”, *Soil Dyn. and Earthq. Eng.*, 26(5), pp. 347-361, 2006.
- [28] Gerolymos, N, Gazetas, G, “Development of Winkler model for static and dynamic response of caisson foundations with soil and interface nonlinearities”, *Soil Dynamics and Earthquake Engineering*, 26, pp. 363-376, 2006.
- [29] Gerolymos, N, Gazetas, G, “Static and dynamic response of massive caisson foundations with soil and interface nonlinearities – validation and results”, *Soil Dynamics and Earthquake Engineering*, 26, pp. 377-394, 2006.
- [30] Varun, Assimaki, D, Gazetas, G, “A simplified model for lateral response of large diameter caisson foundations – Linear elastic formulation”, *Soil Dyn. and Earth. Eng.*, Vol. 29, pp. 268-291, 2009.
- [31] Zhong, R, Huang, M, “Winkler model for dynamic response of composite caisson-piles foundations: Lateral response”, *Soil Dynamics and Earthquake Engineering*, 55, pp. 182-194, 2013.
- [32] Karapiperis, K, Gerolymos, N, “Combined loading of caisson foundations in cohesive soil: Finite element versus Winkler modeling”, *Computers and Geotechnics*, 56, pp. 100-120, 2014.
- [33] Semblat, JF, Pecker, A, *Waves and vibrations in soils: Earthquakes, traffic, shocks, construction works*, IUS Press, Pavia, 2009.
- [34] Wolf, JP, *Dynamic soil-structure interaction*, Prentice-Hall, Englewood Cliffs, N.J., 1985.
- [35] Bard, P-Y, Riepl-ThomasJ, “Wave propagation in complex geological structures and their effects on strong ground motion”, *Wave motion in earthquake engineering*. Kausel &

Manolis (eds), WIT Press, Southampton, pp. 37-95, 2000.

- [36] Gazetas, G, *Foundation vibrations*, Foundation Engineering Handbook, 2nd ed. Y. Fang (ed.), Van Nostrand Reinhold, New York, pp. 553-593, 1991.
- [37] Mylonakis, G, Nikolaou, S, Gazetas, G, "Footings under seismic loading: analysis and design issues with emphasis on bridge foundations", *Soil Dynamics and Earthquake Engineering*, 26, 824-853, 2006.